

HOKKAIDO UNIVERSITY

Title	Combustion Reactions between Transition-Metal Chlorides and Sodium Amide and Their Ignition Temperature
Author(s)	Noguchi, Shinji; Odahara, Jin; Sakai, Hayato et al.
Citation	Inorganic Chemistry, 60(17), 12753-12758 https://doi.org/10.1021/acs.inorgchem.1c00557
Issue Date	2021-08-24
Doc URL	https://hdl.handle.net/2115/100470
Rights	This document is the Accepted Manuscript version of a Published Article that appeared in final form in Combustion Reactions between Transition-Metal Chlorides and Sodium Amide and Their Ignition Temperature, copyright © 2021 American Chemical Society. To access the final published article, see ACS Articles on Request.
Type	journal article
File Information	ShinjiNoguchi2021_InorgChem_60-17_12753-12758.pdf



Hokkaido University Collection of Scholarly and Academic Papers : HUSCAP

Combustion Reactions Between Transition-Metal Chlorides and Sodium Amide and Their Ignition Temperature

Shinji Noguchi,[a] Jin Odahara,[a] Hayato Sakai,[b] Nataly Carolina Rosero-Navarro [b], Akira Miura*[b] and Kiyoharu Tadanaga[b]

[a] Graduate School of Chemical Science and Engineering, Hokkaido University, Kita-13, Nishi-8, Kita-ku,Sapporo, Hokkaido 060-8628.

[b] Faculty of Engineering, Hokkaido University, Kita-13, Nishi-8, Kita-ku, Sapporo, Hokkaido 060-8628.

Corresponding Author: amiura@eng.hokudai.ac.jp

ABSTRACT: Combustion reactions between metal chlorides and sodium amide proceed in a short time; however, these reactions must be carried out with appropriate safety measures. Investigating their ignition temperatures would facilitate safe handling and give kinetic insights of the reaction between powders. Here, we investigated the products of the reactions between metal chlorides and sodium amide and measured their ignition temperatures. The products were mainly composed of nitrides, metals, and sodium chloride. The reactions of 4d and 5d metal chlorides initiated the reaction below room temperature, while 3d metal chlorides except copper chloride initiated the reaction upon heating. We found the correlation between ignition temperature and reaction energies of the combustion reaction.

1. Introduction

Metal nitrides are exciting materials because of their wide range of applications and high performance.[1–3] Typical applications include catalysts[1–3], superconductors[4,5], semiconductors[6,7], magnetic materials[8–10], and super hard materials.[11,12] Nonetheless, their syntheses often require long-term heating at high temperatures,[14] sometimes under high pressure.[15,16] Combustion synthesis is used for synthesizing metal nitrides in a short time. For example, 4d- and 5d-transition metal nitrides, such as NbN, ZrN, and TaN, have been synthesized by combustion reactions between their chlorides and Li_3N.[17] The reaction is highly exothermic, and the reaction often finishes within a second. The reaction enthalpy, heat capacity, heat of fusion, and heat of evaporation can be useful to select the set of precursors.[18]

$NaNH_2$ is another solid nitrogen source for producing nitrides/oxynitrides through the reaction with oxides or chlorides.[16,19–22] Recently, we synthesized novel ternary nitrides such as Mn-Mo-N[23] and perovskite oxynitrides such as $BaNbO_2N$[24] by combustion reactions using $NaNH_2$, which can produce nitrides/oxynitrides in a few seconds. The reaction temperature was controlled by changing the starting materials[23] and by the addition of an organic solvent.[24] Nonetheless, to understand how to handle these highly reactive materials safety, initiation conditions of these reactions should be examined. Moreover, to our knowledge, the combustion synthesis of MnN_x, Fe_3N_x, and Cu_3N has not yet been reported.

Exploration of functional materials is based on try-and-error approaches, but recent computational works are trying to understand and predict reaction routes for the rational design of synthesis reactions. Although the design of solid-state reactions is still challenging due to competing for thermodynamic and kinetic factors, there are achievements for understanding and predicting synthesis routes. The examples of understanding reaction pathways via thermodynamic driving force are that the first reaction proceeds with locally consuming large thermodynamic energies.[26,27] Graph-based theory can derive likely reaction pathways by using thermodynamic reaction energies as cost functions.[28] Another example using kinetics nucleation barriers also proposed likely reaction routes.[29] In this model, the nucleation barriers are calculated by surface energy, interface mismatch, and bulk formation energy calculated by DFT calculation; large reaction energy is favorable for proceeding reactions. Even though the above models do not entirely include thermodynamic and kinetic factors, these successful examples suggest that large reaction energy can satisfy fast kinetic requirements. Nonetheless, the experimental work for the correlation between reaction energy and activation energy is still limited; classical works in 1930th about the reactions with molecules can explain the correlation between their trends.[30,31] Combustion reactions from solid particles are fast solid-state reactions. Thus, these reactions can be candidates for evaluating the correlation between thermodynamic reaction energies and the kinetic factor to start solid-state reactions.

In this study, we examined the reaction between metal chlorides and $NaNH_2$ for the formation of nitrides/metals, and measured their ignition temperature. The correlation between the ignition temperature and thermodynamic parameters was investigated.

2. Experimental Section

MCl_x (**$CrCl_3$**, Aldrich, 99%; **$MnCl_2$**, Strem Chemicals, 97%; **$FeCl_2$**, Strem Chemicals, 98%, **VCl_3**, Aldrich, 97%; **$CuCl_2$**, Wako, 95%; **$NbCl_5$**, Kanto, 99%; **$MoCl_3$**, Aldrich, 99.5%; **$MoCl_5$**, Wako, 99.5%; **$TaCl_5$**, Kanto, 95%; **WCl_4**, Aldrich, 95%; **WCl_6**, Aldrich, 99.9%;) were ground in a mortar and pestle for 10 min in an argon-filled glove box with dew point of approximately −90 °C with particle sizes of approximately 10–50 μm (Figure

S1). The glovebox was used for the experiment under an inert gas atmosphere. The Teflon-lined autoclave (Yanako, AD-70) with an inner volume of 70 mL was heated at 493 K overnight to remove any water before the synthesis reaction of metal nitrides. ***Caution!*** *An intense exothermic reaction occurs as soon as these powders are mixed. Synthesis using a large amount of the starting materials may cause a serious accident. The total mass of these powders was less than 700 mg. Wear protective glasses during the experiment.*

The screening of reactivity was performed by mixing metal chlorides and $NaNH_2$ at room temperature. First, 1 mmol of transition metal chloride powder and a magnetic stirrer were added to the autoclave, and then, 10 mmol of white $NaNH_2$ powder (Aldrich, 98%) was added. Magnetic stirring was conducted for 1 min to mix the powders in the closed autoclave. XRD profiles of the products were measured using Cu Ka (Rigaku, Miniflex600) before and after washing with water and dried at 323 K. The amounts of oxygen and nitrogen in the product were measured by the combustion analyzer (EMGA-620, Horiba).

Ignition temperatures of the reaction between metal chlorides and $NaNH_2$ were measured by two approaches, depending on the screening described above. The first approach was for the powder mixture that did not react at room temperature. One spatula of the mixed powder (~0.01 mg) was heated by a microheater in an argon atmosphere. The temperature of the sample was increased from room temperature at the rate of 1 K/s. A sudden explosive reaction occurred upon heating and the white powder changed to black (Figure S2). The temperature at which the explosive reaction occurs was defined as the ignition temperature, and the ignition temperature of the mixed powder containing each metal chloride was measured. The other approach was for the powder mixture that reacted at room temperature. Chloride powder (0.05 mmol), $NaNH_2$ powder (0.5 mmol), and a magnetic stirrer were placed in a glass vessel and sealed using a plastic lid. The bottle was cooled down to 173 K by a low-temperature bath. The cooler was turned off and the temperature was naturally increased at 5–10 K/min (Figure S3). Each measurement was performed three to six times.

3. Results and Discussion

The products of the reactions between $NaNH_2$ and transition metal chlorides were characterized by XRD: WCl_6, WCl_4, $TaCl_5$, $MoCl_5$, $MoCl_3$, $NbCl_5$, $CuCl_2$, $FeCl_2$, $MnCl_2$, $CrCl_3$, and VCl_3. Before washing with water, the diffraction peaks of NaCl were clear but other peaks were weak (Figure S4). Thus, XRD patterns after washing with water were shown in Figure 1 except $FeCl_2$; the pattern of $FeCl_2$ was shown before washing with water because washing with water completely decomposes Fe_3N_x.[32] The diffraction peaks of nitrides were observed in all the cases. The lattice parameters of nitrides were summarized in Table S1. Those of Fe_3N_x, Cu_3N, and VN were rather weak. Moreover, in addition to nitrides, we can see the diffraction peaks of metals, oxides, and other unindexed peaks. Exhibiting the diffraction peaks of metals and other unindexed peaks may be related to the low decomposition temperature of Fe_3N_x,[33] Cu_3N,[34] and VN.[35] The nitrogen and oxygen content were quantitatively evaluated by combustion analysis (Table S2). All products contained nitrogen and oxygen. The products were likely oxidized when they were exposed to air and water. Specifically, Cu_2O, and CuO are probably formed by washing with water, considering no diffraction peaks before washing (Figure S4). $NaTaO_3$ may form from Ta source with $NaNH_2$ considering the exothermic reaction of $NaNH_2$ with water during washing.[36]

The corresponding reaction formulas to produce nitrides/metals from each metal chlorides are listed in Table 1. The reaction mechanism to produce both nitrides and metals is not completely understood because XRD patterns show the diffraction peaks of not only nitrides but also metals and other phases.

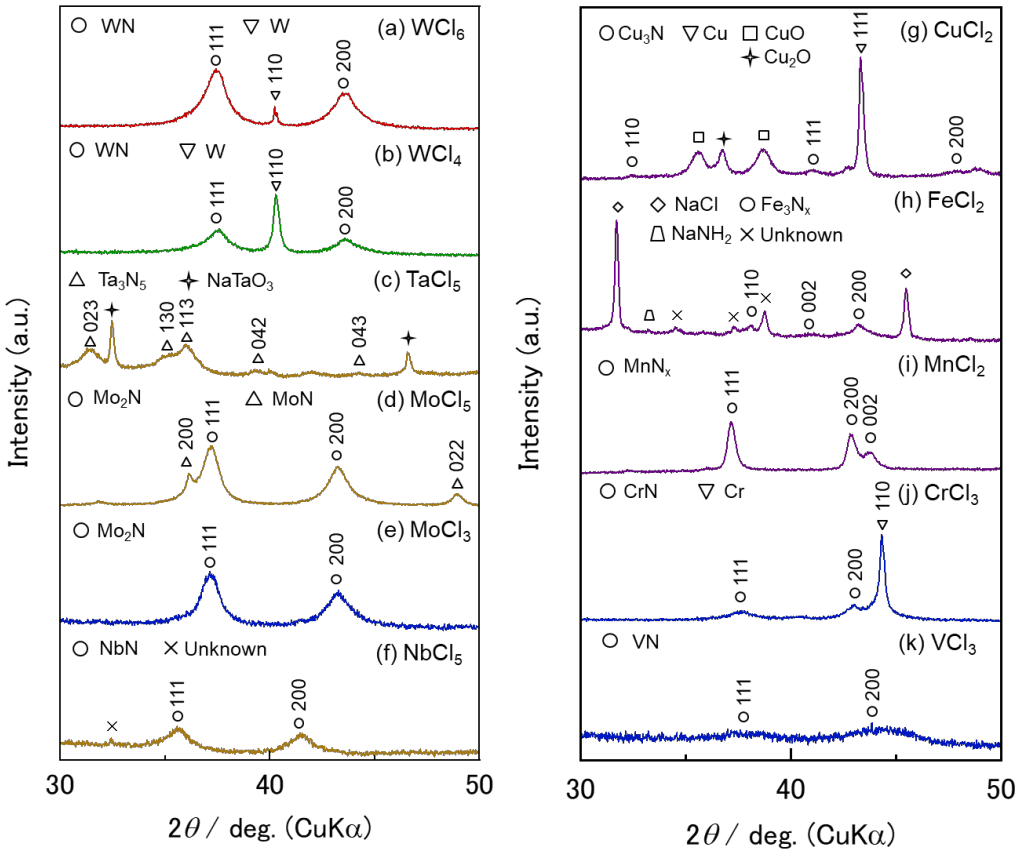


FIGURE 1 XRD patterns of products using $NaNH_2$ and (a) WCl_6, (b) WCl_4, (c) $TaCl_5$, (d) $MoCl_5$, (e) $MoCl_3$, (f) $NbCl_5$, (g) $CuCl_2$, (h) $FeCl_2$, (i) $MnCl_2$, (j) $CrCl_3$, (k) VCl_3, after washing. Please note that only the XRD pattern of (h) $FeCl_2$ is the product before washing and dried at 323 K.

TABLE 1 Reaction formula for producing nitrides/metal from chlorides and sodium amides and corresponding ΔH_{rxn} calculated using references.[38,39]

Reaction formula	ΔH_{rxn} / kJ
$WCl_6+6NaNH_2 \rightarrow WN+6NaCl+4NH_3+1/2N_2$	−1358
$WCl_6+6NaNH_2 \rightarrow W+6NaCl+4NH_3+N_2$	−1343
$MoCl_5+5NaNH_2 \rightarrow 1/2Mo_2N+5NaCl+10/3NH_3+7/12N_2$	−1108
$MoCl_5+5NaNH_2 \rightarrow Mo+5NaCl+10/3NH_3+5/6N_2$	−1188
$NbCl_5+5NaNH_2 \rightarrow NbN+5NaCl+10/3NH_3+1/3N_2$	−1053
$NbCl_5+5NaNH_2 \rightarrow Nb+5NaCl+10/3NH_3+5/6N_2$	−817
$TaCl_5+5NaNH_2 \rightarrow 1/3Ta_3N_5+5NaCl+10/3NH_3$	−1039
$TaCl_5+5NaNH_2 \rightarrow Ta+5NaCl+10/3NH_3+5/6N_2$	−756
$WCl_4+4NaNH_2 \rightarrow WN+4NaCl+8/3NH_3+1/6N_2$	−864
$WCl_4+4NaNH_2 \rightarrow W+4NaCl+8/3NH_3+2/3N_2$	−849
$MoCl_3+3NaNH_2 \rightarrow 1/2Mo_2N+3NaCl+2NH_3+1/4N_2$	−717
$MoCl_3+3NaNH_2 \rightarrow Mo+3NaCl+2NH_3+1/2N_2$	−697
$VCl_3+3NaNH_2 \rightarrow VN+3NaCl+2NH_3$	−605
$VCl_3+3NaNH_2 \rightarrow V+3NaCl+2NH_3+1/2N_2$	−388
$CrCl_3+3NaNH_2 \rightarrow CrN+3NaCl+2NH_3$	−516
$CrCl_3+3NaNH_2 \rightarrow Cr+3NaCl+2NH_3+1/2N_2$	−398
$FeCl_2+2NaNH_2 \rightarrow 1/3Fe_3N+2NaCl+4/3NH_3+1/6N_2$	−308
$FeCl_2+2NaNH_2 \rightarrow Fe+2NaCl+4/3NH_3+1/3N_2$	−304
$MnCl_2+2NaNH_2 \rightarrow 1/3Mn_3N_2+2NaCl+4/3NH_3$	−208
$MnCl_2+2NaNH_2 \rightarrow Mn+2NaCl+4/3NH_3+1/3N_2$	−165
$CuCl_2+2NaNH_2 \rightarrow 1/3Cu_3N+2NaCl+4/3NH_3+1/6N_2$	−405
$CuCl_2+2NaNH_2 \rightarrow Cu+2NaCl+4/3NH_3+1/3N_2$	−430

To handle the reaction safely and understand the reaction mechanism, we measured the ignition temperature of the reaction between chlorides and $NaNH_2$, and investigated the correlation between the ignition temperature and the physical parameters. The evaluation of critical factors determining the ignition temperature should be very carefully considered because the reaction products are not fully characterized and the number of chloride species is limited. Thus, we qualitatively evaluate the correlation between ignition temperature and various physical properties and discuss the factor that likely affects ignition temperature.

We evaluate the relationship of reaction enthalpies, the valence of chlorides, and the vapor pressure of chlorides by using Pearson correlation coefficient. The Pearson correlation coefficient, *R*, between 0 and 0.3, between 0.3 and 0.7, and between 0.7 and 1.0 indicate a weak, moderate, and strong positive linear relationship, respectively.[40] Figures 2(a) and (b) show the relationship between the reaction enthalpies of the chemical reaction formula for producing nitrides and metals (Table 1) and the ignition temperatures of the combustion reactions. Figure 2(c) exhibits the correlation of the valence of metal chlorides, and Figure 2(d) displays that of the vapor pressure and the metal chlorides.

Two models were employed to evaluate various physics parameters. The first one is the total model for considering all the chlorides. The second one is the separate model for considering 3d metal chlorides without $CuCl_2$ which initiate above room temperature and 4d-5d metals with $CuCl_2$ that initiate at or below room temperature, respectively. In the total model, there are strong linear relationships between ignition temperature and reaction enthalpies for the formation of nitrides/metals and metal chloride valence. In the separate model, there are moderate or weak linear relationships between the ignition temperature and the reaction enthalpies for the formation of nitrides/metals, and between the ignition temperature and metal chloride valence. In the case of the second model, there are linear relationships but the correlation is weak. While the correlations of reaction enthalpies with the ignition temperatures are positive, the correlation of the metal valence is negative. The similar correlation factors between the reaction energies for the formation of nitrides (Figure 2 (a)) and metals (Figure 2(b)) is attributed to the fact that the driving force of these reactions is mainly attributed to sodium chlorides, not nitrides/metals.

High valence tends to decrease reaction enthalpy (|Δ*H*| become large) because of the large formation energy of NaCl. Thus, it is natural to consider that these positive correlations are mainly attributed to the formation energy of NaCl, which is the main thermodynamic driving force of these combustion reactions. The reason for the discontinuity of the linear fitting of the separate model may be attributed to the existence of a gap of reaction enthalpy facilitating ignitions.

The vapor pressure has a moderate negative linear relationship with ignition temperatures in the total model and the 4d-5d metals with $CuCl_2$ of the separate model. This negative relationship suggests that solid-vapor reaction is unlikely because the high vapor pressure enhances the reaction kinetics of this reaction mechanism. Thus, we believe that the solid-solid reactions between chlorides and sodium amide are dominant for starting reaction, not solid-vapor reaction.

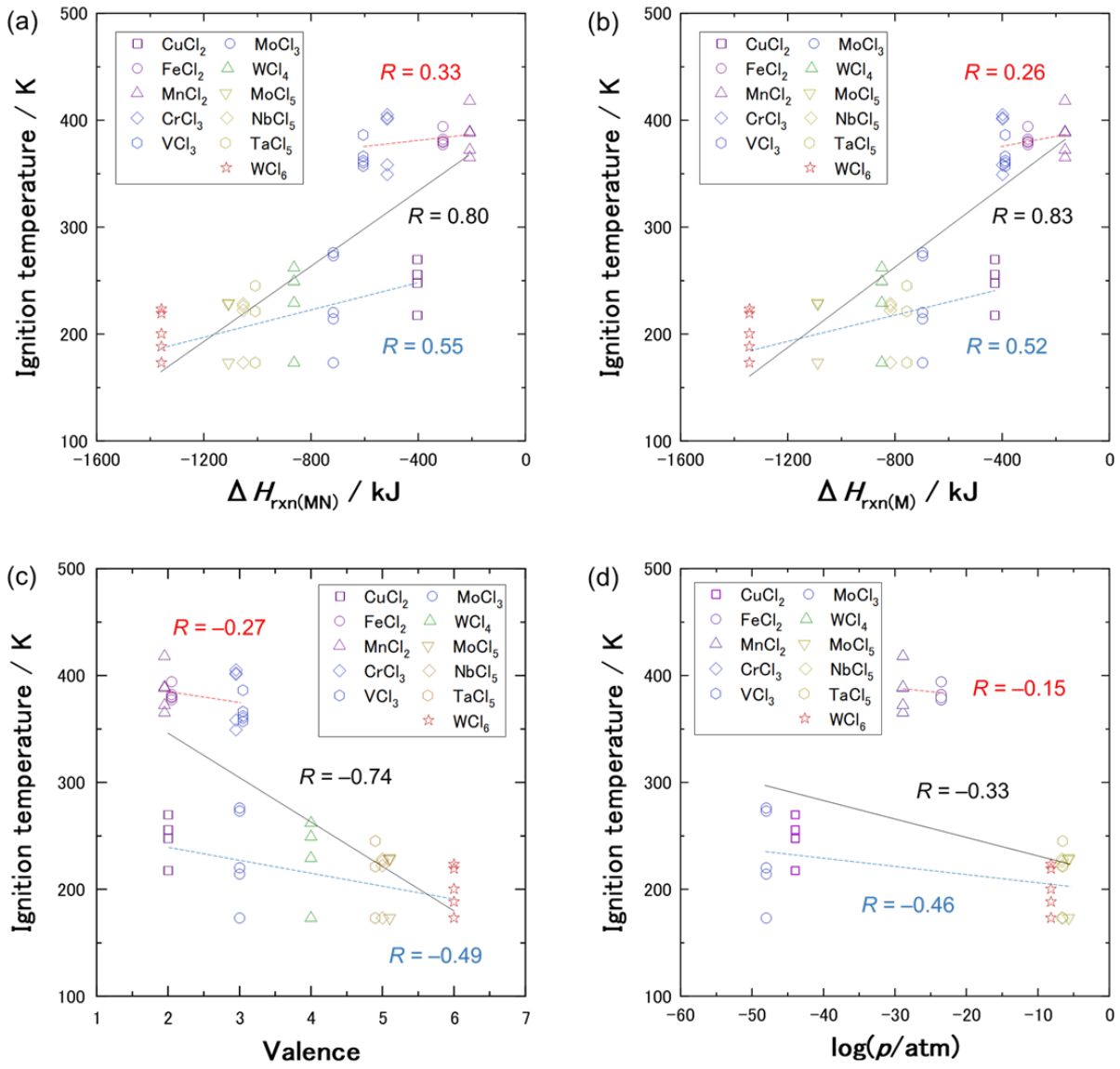


FIGURE 2 (a) Relationship between reaction enthalpy to produce nitrides and ignition temperature of the reaction. (b) Relationship between reaction enthalpy to produce metals and ignition temperature of the reaction. (c) Relationship between the valence of metal chlorides and ignition temperature of the reaction. (d) Relationship between vapor pressures and ignition temperature of the reaction. Black lines represent the linear fitting of the total model, and red and blue lines represent the linear fitting of the separate model. The Pearson correlation coefficient, *R*, between 0 and 0.3, between 0.3 and 0.7, and between 0.7 and 1.0 indicate a weak, moderate and strong positive linear relationship, respectively.[40]

It should be mentioned that the ignition temperature of $CuCl_2$ deviates from the trend in the total model and locates in the group of 4d-5d metals in the separate model. This would be explained by the difference in the local structures of metal chlorides. $CuCl_2$ has a square planar Cu-Cl_4 geometry[41] while other metal chlorides have an M-Cl_6 octahedral structure, where M represents metal. $NaNH_2$ can contact both metal and chloride ions in the four-coordinated geometry, while it can touch only chloride ions in the octahedral geometry (Figure 3). Thus, lower reaction temperatures of $CuCl_2$ and $NaNH_2$ suggest that the reaction mechanism also depends on the local geometry.

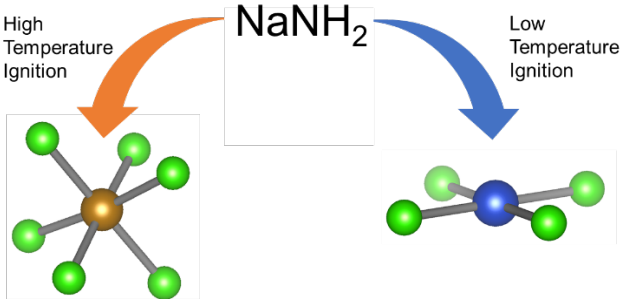


Figure 3 Schematic illustrations of the reaction of six-coordinated chlorides and four-coordinated chlorides.

By considering nitrogen amounts as an evaluation factor for the formation of nitrides, the relationship between the nitrogen content of the products and various parameters such as the reaction enthalpy for the formation of nitrides/metals, the valence of the metal chloride, and the ignition temperature was evaluated (Figure S5). However, only weak linear correlations were found.

The ignition temperature of combustion reactions was found to be correlated with their large reaction energy. Once a highly ectothermic reaction proceeds from the solid-solid interface, the reaction accelerates by $NaNH_2$ melting or gas generation of N_2/NH_3. Assuming that the thermal energy proportional to temperature overcomes the activation energies of the reactions, the Bell-Evans-Polanyi principle,[30,31] inclination that the activation energy is proportional to the enthalpy of reaction, can be applied to the combustion reaction.

Combustion reactions are highly exothermic and are considered to be a motif of solid-state reactions for evaluating the correlation between thermodynamic reaction energies and the kinetic factor to start solid-state reactions. As described in the introduction, recent computational works successfully proposed likely solid-state reaction candidates using computationally calculated thermodynamic data with simplified kinetic consideration or even without considering kinetic factors. These works are based on the assumption that reaction with large thermodynamic can proceed with smaller kinetic barriers. Although reactions with relatively small thermodynamic driving forces are not the targets of this work, the experimental result with highly exothermic reactions shown here can support the correlation of thermodynamic driving force and kinetic barrier in solid-state reaction, guiding the design of solid-state reaction by using thermodynamic driving force.

4. Conclusions

The reaction of various transition metal chlorides and sodium amide initiated a highly exothermic metathesis reaction to form nitrides, metals, and sodium chlorides. The ignition temperature of 4d-5d transition metal chlorides was below 273 K whereas that of 3d transition chlorides except $CuCl_2$ was 350-420 K. A linear relationship was found between the reaction enthalpies forming nitrides/metals and the ignition temperature of the combustion reaction. We believe that this study facilitates the understanding of the safety requirements of highly reactive materials and for guiding the reaction principles by the relationships between reaction energy and reaction kinetics in solid-state reactions.

ASSOCIATED CONTENT

AUTHOR INFORMATION

Corresponding Author

Akira Miura: amiura@eng.hokudai.ac.jp

ACKNOWLEDGMENT

We thank Profs. Satoshi Maeda and Taisuke Hasegawa (Hokkaido Univ.) for discussion about activation energies of the combustion reactions. This research was partially supported by KAKENHI Grant Numbers JP17H04950, JP19H04682 and JP21H02022.

Supporting Information

The lattice constants of synthesized nitrides, the nitrogen and oxygen contents of the products, SEM images of starting materials, photos of self-combustion synthesis, XRD patterns before washing with water, and the relationship between the nitrogen content and various parameters are in the supporting information.

REFERENCES

(1) Yuan, Y.; Wang, J.; Adimi, S.; Shen, H.; Thomas, T.; Ma, R.; Attfield, J. P.; Yang, M. Zirconium Nitride Catalysts Surpass Platinum for Oxygen Reduction. *Nat. Mater.* **2019**, *19* (March). https://doi.org/10.1038/s41563-019-0535-9.

(2) Ojha, K.; Saha, S.; Kumar, B.; Hazra, K. S.; Ganguli, A. K. Controlling the Morphology and Efficiency of Nanostructured Molybdenum Nitride Electrocatalysts for the Hydrogen Evolution Reaction. *ChemCatChem* **2016**, *8* (6), 1218–1225. https://doi.org/10.1002/cctc.201501341.

(3) McGee, R. C. V.; Thompson, L. T. Nature of Acid-Base Sites on Molybdenum Nitride Catalysts: Effect of Nitrogen and Oxygen Content. *Appl. Catal. A Gen.* **2020**, *605*, 117777. https://doi.org/10.1016/j.apcata.2020.117777.

(4) Keskar, K. S.; Yamashita, T.; Onodera, Y. Superconducting Transition Temperatures of r. F. Sputtered Nbn Films. *Jpn. J. Appl. Phys.* **1971**, *10* (3), 370–374. https://doi.org/10.1143/JJAP.10.370.

(5) Yamanaka, S. Intercalation and Superconductivity in Ternary Layer Structured Metal Nitride Halides (MNX: M = Ti, Zr, Hf; X = Cl, Br, I). *J. Mater. Chem.* **2010**, *20* (15), 2922–2933. https://doi.org/10.1039/b922149b.

(6) Nayak, C.; Palai, G.; Sarkar, P. Investigation of Mole Fraction in Nitride Semiconductor Using Photonic Bandgap Analysis. *Optik (Stuttg).* **2016**, *127* (2), 697–699. https://doi.org/10.1016/j.ijleo.2015.10.131.

(7) Bauers, S. R.; Holder, A.; Sun, W.; Melamed, C. L.; Woods-Robinson, R.; Mangum, J.; Perkins, J.; Tumas, W.; Gorman, B.; Tamboli, A.; Ceder, G.; Lany, S.; Zakutayev, A. Ternary Nitride Semiconductors in the Rocksalt Crystal Structure. *Proc. Natl. Acad. Sci.* **2019**, *116* (30), 14829–14834. https://doi.org/10.1073/PNAS.1904926116.

(8) Li, X.; Sun, X.; Wang, J.; Liu, Q. Microstructure and Magnetic Properties of Iron Nitride Thin Films. *J. Alloys Compd.* **2014**, *582*, 398–402. https://doi.org/10.1016/j.jallcom.2013.08.064.

(9) Mi, W. B.; Feng, X. P.; Duan, X. F.; Yang, H.; Li, Y.; Bai, H. L. Microstructure, Magnetic and Electronic Transport Properties of Polycrystalline Γ′-Fe 4N Films. *Thin Solid Films* **2012**, *520* (23), 7035–7040. https://doi.org/10.1016/j.tsf.2012.07.053.

(10) Yamashita, S.; Masubuchi, Y.; Nakazawa, Y.; Okayama, T.; Tsuchiya, M.; Kikkawa, S. Crystal Structure and Magnetic Properties of A′′-Fe 16N 2 Containing Residual α-Fe Prepared by Low-Temperature Ammonia Nitridation. *J. Solid State Chem.* **2012**, *194*, 76–79. https://doi.org/10.1016/j.jssc.2012.07.025.

(11) Vieira, M. T.; Ramos, A. S. Influence of Ductile Interlayers on the Mechanical Performance of Tungsten Nitride Coatings. *J. Mater. Process. Technol.* **1999**, *92–93*, 156–161. https://doi.org/10.1016/S0924-0136(99)00235-6.

(12) Paseuth, A.; Yamagata, K.; Miura, A.; Higuchi, M.; Tadanaga, K. Deposition and Analysis of Al-Rich c-AlxTi1−xN Coating with Preferred Orientation. *J. Am. Ceram. Soc.* **2017**, *100* (1), 343–353. https://doi.org/10.1111/jace.14549.

(13) Rasaki, S. A.; Zhang, B.; Anbalgam, K.; Thomas, T.; Yang, M. Synthesis and Application of Nano-Structured Metal Nitrides and Carbides: A Review. *Progress in Solid State Chemistry*. Elsevier Ltd June 1, 2018, pp 1–15. https://doi.org/10.1016/j.progsolidstchem.2018.05.001.

(14) S. Bem, D.; M. Lampe-Önnerud, C.; P. Olsen, H.; zur Loye, H.-C. Synthesis and Structure of Two New Ternary Nitrides: FeWN2 and MnMoN2. *Inorg. Chem.* **1996**, *35* (3), 581–585. https://doi.org/10.1021/ic9512338.

(15) Zerr, A.; Miehe, G.; Li, J.; Dzivenko, D. A.; Bulatov, V. K.; Höfer, H.; Boifan-Casanova, N.; Fialin, M.; Brey, G.; Watanabe, T.; Yoshimura, M. High-Pressure Synthesis of Tantalum Nitride Having Orthorhombic U 2S3 Structure. *Adv. Funct. Mater.* **2009**, *19* (14), 2282–2288. https://doi.org/10.1002/adfm.200801923.

(16) Miura, A. Low-Temperature Synthesis and Rational Design of Nitrides and Oxynitrides for Novel Functional Material Development. *J. Ceram. Soc. Japan* **2017**, *125* (7), 552–558.

(17) Gillan, E. G.; Kaner, R. B. Synthesis of Refractory Ceramics via Rapid Metathesis Reactions between Solid-State Precursors. *Chem. Mater.* **1996**, *8* (2), 333–343. https://doi.org/10.1021/cm950232a.

(18) Wiley, J. B.; Kaner, R. B. Rapid Solid-State Precursor Synthesis of Materials. *Science (80-.).* **1992**, *255* (5048), 1093–1097. https://doi.org/10.1126/science.255.5048.1093.

(19) Miura, A.; Takei, T.; Kumada, N. Synthesis of Wurtzite-Type InN Crystals by Low-Temperature Nitridation of LiInO2 Using NaNH2 Flux. *Cryst. Growth & Des.* **2012**, *12* (9), 4545–4547. https://doi.org/10.1021/cg3007266.

(20) Miura, A.; Takei, T.; Kumada, N. Low-Temperature Nitridation of Manganese and Iron Oxides Using NaNH2 Molten Salt. *Inorg. Chem.* **2013**, *52* (20), 11787–11791. https://doi.org/10.1021/ic401951u.

(21) Miura, A.; Takei, T.; Kumada, N. Synthesis of Cu 3 N from CuO and NaNH 2. *Journal of Asian Ceramic*

Societies. Elsevier B.V. December 1, 2014, pp 326–328. https://doi.org/10.1016/j.jascer.2014.08.007.

(22) E. O'Sullivan, S.; Sun, S.-K.; M. Lawson, S.; C. Stennett, M.; Chen, F.; Masubuchi, Y.; L. Corkhill, C.; C. Hyatt, N. Low-Temperature Nitridation of Fe3O4 by Reaction with NaNH2. *Inorg. Chem.* **2021**, *60* (4), 2553–2562. https://doi.org/10.1021/acs.inorgchem.0c03452.

(23) Odahara, J.; Sun, W.; Miura, A.; Carolina Rosero-Navarro, N.; Nagao, M.; Tanaka, I.; Ceder, G.; Tadanaga, K. Self-Combustion Synthesis of Novel Metastable Ternary Molybdenum Nitrides. *ACS Mater. Lett.* **2019**, *1* (1), 64–70. https://doi.org/10.1021/acsmaterialslett.9b00057.

(24) Odahara, J.; Miura, A.; Rosero-Navarro, N. C.; Tadanaga, K. Explosive Reaction for Barium Niobium Perovskite Oxynitride. *Inorg. Chem.* **2017**, *57* (1), 24–27. https://doi.org/10.1021/acs.inorgchem.7b02660.

(25) Jain, A.; Ong, P.; Hautier, G.; Chen, W.; Richards, W. D.; Dacek, S.; Cholia, S.; Gunter, D.; Skinner, D.; Ceder, G.; Persson, K. A. Commentary: The Materials Project: A Materials Genome Approach to Accelerating Materials Innovation. *APL Mater.* **2013**, *1*, 11002. https://doi.org/10.1063/1.4812323.

(26) Bianchini, M.; Wang, J.; Clément, R. J.; Ouyang, B.; Xiao, P.; Kitchaev, D.; Shi, T.; Zhang, Y.; Wang, Y.; Kim, H.; Zhang, M.; Bai, J.; Wang, F.; Sun, W.; Ceder, G. The Interplay between Thermodynamics and Kinetics in the Solid-State Synthesis of Layered Oxides. *Nat. Mater.* **2020**, *19* (10), 1088–1095. https://doi.org/10.1038/s41563-020-0688-6.

(27) Miura, A.; Bartel, C. J.; Goto, Y.; Mizuguchi, Y.; Moriyoshi, C.; Kuroiwa, Y.; Wang, Y.; Yaguchi, T.; Shirai, M.; Nagao, M.; Rosero-Navarro, C.; Tadanaga, K.; Ceder, G.; Sun, W.; Miura, A.; Rosero-Navarro, C.; Tadanaga, K.; Bartel, C. J.; Ceder, G.; Goto, Y.; Mizuguchi, Y.; Moriyoshi, C.; Kuroiwa, Y.; Wang, Y.; Yaguchi, T.; Shirai, M.; Nagao, M.; Sun, W. Observing and Modeling the Sequential Pairwise Reactions That Drive Solid-State Ceramic Synthesis. *Adv. Mater.* **2021**, *33* (24). https://doi.org/10.1002/adma.202100312.

(28) McDermott, M. J.; Dwaraknath, S. S.; Persson, K. A. A Graph-Based Network for Predicting Chemical Reaction Pathways in Solid-State Materials Synthesis. *Nat. Commun.* **2021**, *12* (1), 3097. https://doi.org/10.1038/s41467-021-23339-x.

(29) Aykol, M.; Montoya, J. H.; Hummelshøj, J. S.; Aykol, M.; Montoya, J. H.; Hummelshøj, J. Rational Solid-State Synthesis Routes for Inorganic Materials Rational Solid-State Synthesis Routes for Inorganic Materials. **2021**, No. 2. https://doi.org/10.26434/chemrxiv.13546484.v1.

(30) Onald, R.; Bell, P. The Theory of Reactions Involving Proton Transfers. *Prodeecing R. Soc. A* **1936**, *154* (882), 414–429.

(31) Evans, M. G.; Polanyi, M. FURTHER CONSIDERATIONS ON THE THERMO-DYNAMICS OF CHEMICAL EQUILIBRIA AND REACTION RATES. *Trans. Faraday Soc.* **1936**, *32*, 1333–1360.

(32) Miura, A.; Takei, T.; Kumada, N. Low-Temperature Nitridation of Manganese and Iron Oxides Using NaNH2 Molten Salt. *Inorg. Chem.* **2013**, *52* (20), 11787–11791. https://doi.org/10.1021/ic401951u.

(33) Wu, X. L.; Zhong, W.; Tang, N. J.; Jiang, H. Y.; Liu, W.; Du, Y. W. Magnetic Properties and Thermal Stability of Nanocrystalline ε-Fe 3N Prepared by Gas Reduction-Nitriding Method. *J. Alloys Compd.* **2004**, *385* (1–2), 294–297. https://doi.org/10.1016/j.jallcom.2004.04.127.

(34) Masaaki Asano; Kazuo Umeda; Akira Tasaki. Cu3N Thin Film for a New Light Recording Media. *Jpn. J. Appl. Phys.* **1990**, *29*, 1985.

(35) Gajbhiye, N. S.; Ningthoujam, R. S. Low Temperature Synthesis, Crystal Structure and Thermal Stability Studies of Nanocrystalline VN Particles. *Mater. Res. Bull.* **2006**, *41* (9), 1612–1621. https://doi.org/10.1016/j.materresbull.2006.02.036.

(36) Li, X.; Zang, J. Facile Hydrothermal Synthesis of Sodium Tantalate (NaTaO3) Nanocubes and High Photocatalytic Properties. *J. Phys. Chem. C* **2009**, *113* (45), 19411–19418. https://doi.org/10.1021/jp907334z.

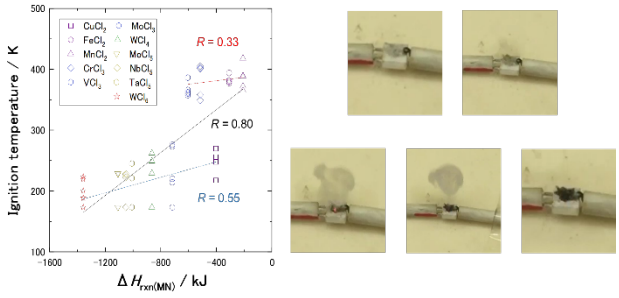
(37) Archer, D. G. Thermodynamic Properties of the NaCl+H 2 O System l. Thermodynamic Properties of NaCl(Cr). *Aqueous Sodium Chloride Solut. J. Phys. Chem. Ref. Data* **1992**, *21*, 15. https://doi.org/10.1063/1.555915.

(38) Höhn, P.; Niewa, R. Nitrides of Non-Main Group Elements. *Handb. Solid State Chem.* **2017**, *2*, 251–359. https://doi.org/10.1002/9783527691036.hsscvol1008.

(39) Daubert, T. E.; Danner, R. P. Physical and Thermodynamic Properties of Pure Chemicals: Data Compilation. *Choice Rev. Online* **1990**, *27* (06), 27-3319-27–3319. https://doi.org/10.5860/choice.27-3319.

(40) Bruce Ratner. The Correlation Coefficient: Its Values Range between +1/−1, or Do They? *J. Targeting, Meas. Anal. Mark.* **2009**, *17*, 139–142. https://doi.org/10.1057/jt.2009.5.

(41) F Wells, B. A. The Crystal Structure of Anhydrous Cupric Chloride, and the Stereochemistry of the Cupric Atom. *J. Chem. Soc.* **1947**, No. 0, 1670–1675.



We investigated the reactions between metal chlorides and sodium amide and measured their ignition temperatures. The products were composed of nitrides, metals, and sodium chloride. The reactions of 4d/5d metal chlorides and copper chloride with sodium amide initiated the reaction below room temperature, while those of 3d metal chlorides except copper chloride initiated the reaction upon heating. We found that the correlation between ignition temperature and reaction energies of the combustion reactions.